Effect of Initial Swirl Distribution on the Evolution of a Turbulent Jet

S. Farokhi* and R. Taghavi†
University of Kansas, Lawrence, Kansas
and
E. J. Rice‡
NASA Lewis Research Center, Cleveland, Ohio

An existing cold-jet facility at NASA Lewis Research Center was modified to produce swirling flows with controllable initial tangential velocity distribution. Distinctly different swirl velocity profiles were produced, and their effects on jet mixing characteristics were measured downstream of an 11.43 cm (4.5 in.) diameter convergent nozzle. It was experimentally shown that in the near field (i.e., $x/D < 5$) of a swirling turbulent jet, the mean velocity field strongly depends on the initial swirl profile. Two extreme tangential velocity distributions (i.e., one with solid-body rotation and the other predominated by a free-vortex distribution) were produced. The two jets shared approximately the same initial mass flow rate of 0.59 kg/s (1.3 lb/s), mass-averaged axial Mach number ($M_0 = 0.14$), and swirl number ($S = 0.48$). Mean centerline velocity decay characteristics of the solid-body rotation jet flow exhibited classical decay features of a swirling jet with $S = 0.48$ reported in the literature. However, the predominantly free-vortex distribution case (with $S = 0.48$) was on the verge of vortex breakdown, a phenomenon associated with the rotating flows of significantly higher swirl numbers, i.e., $S_{crit} \geq 0.6$. This remarkable result leads to the conclusion that the integrated swirl effect, reflected in the swirl number, is inadequate in describing the mean swirling jet behavior in the near field. The relative size (i.e., diameter) of the vortex core emerging from the nozzle and the corresponding tangential velocity distribution are the controlling parameters influencing the swirling turbulent free-jet evolution.

Nomenclature

A,B,C	= outer, middle, and inner swirl-generating manifolds, respectively
c	= constant
D	= nozzle exit diameter
G	= degree of swirl, $\equiv W_{m0}/U_{m0}$
G_x	= axial flux of axial momentum
G_θ	= axial flux of angular momentum
M	= mean axial Mach number (based on the mass-averaged axial velocity)
$\mathcal{O}$	= order of
p	= static pressure
R	= nozzle exit radius
S	= swirl number, $\equiv G_\theta/G_x R$
U,V,W	= mean axial, radial, and tangential velocity components in the jet, respectively
u',v',w'	= fluctuating axial, radial, and tangential velocity components in the jet, respectively
x,r,θ	= cylindrical polar coordinates in the jet
ϵ	= very small quantity
ρ	= fluid density

Subscripts

crit	= critical
m	= maximum
x	= quantity along the jet centerline
0	= initial value, (i.e., condition at $x/D = 0$)
∞	= unperturbed, ambient condition

Received March 30, 1988; presented as Paper 88-3592 at the First National Fluid Dynamics Congress, Cincinnati, OH, July 25-28, 1988; revision received Aug. 15, 1988.

*Associate Professor, Aerospace Engineering Department.
†Research Associate, Center for Research, Inc.
‡Deputy Chief, Aerodynamics Branch.

Introduction

TURBULENT jets with swirl exhibit distinctive characters absent in their nonrotating counterparts. A subsonic swirl-free jet, for example, experiences theoretically no static pressure gradient in the axial or radial direction. Hence, in this case, the mechanism for jet spread is dominated by the turbulent mixing at the interface between the jet and the ambient fluid. On the other hand, a turbulent jet with strong swirl is primarily driven in the near field ($x/D < 5$) by the static pressure gradients in both axial and radial directions, i.e., mainly an inviscid phenomenon. Turbulent mixing then becomes a dominant factor only when the strong pressure gradients are weakened through rapid initial jet spread (i.e., a jet in near pressure equilibrium). The occurrence of flow reversal in the jet, or what is known as vortex breakdown, is a fascinating phenomenon observed in high-intensity swirling flows, which we will briefly discuss in this paper. The absence of a potential core in a swirling jet is, by definition, another feature that distinguishes the rotating from the nonrotating jets.

The nondimensional parameter describing the integrated swirl strength in a jet is the swirl number S and is defined as

$$S \equiv G_\theta/G_x R \tag{1}$$

where the jet torque is

$$G_\theta \equiv 2\pi \int_0^\infty \rho U W r^2 \, dr \tag{2}$$

the jet axial thrust is

$$G_x \equiv 2\pi \int_0^\infty [\rho U^2 + (p - p_\infty)] r \, dr \tag{3}$$

and R is the nozzle exit radius. The inclusion of the turbulent shear and normal stresses, $\rho \overline{u'w'}$ and $\rho \overline{u'^2}$, in the integrands of the jet torque and thrust expressions [i.e., Eqs. (2) and (3), respectively] provide for total jet thrust and torque as described in Ref. 1. The type of instrumentation used in our

experiment (five-hole pitot probe and single hot-wire anemometer) and the three-dimensional character of swirling turbulent jets did not allow the measurement of radial distribution of Reynolds stresses $\rho\ \overline{u'w'}$ and $\rho\ \overline{u'^2}$ at the nozzle exit. Hence, our swirl number definition excludes the Reynolds stresses. This seems to be a consistent approximation to the swirl number, however, in light of its wide use in the literature (e.g., Refs. 1, 3, 4, 11, 13, 14, and 27). By definition, the swirl number is an integrated quantity; hence, it is possible to generate swirling jets with different initial tangential velocity profiles ranging from solid-body rotation [i.e., $W_0(r) = c \cdot r$] to near free-vortex flow [i.e., $W_0(r) \approx c/r$] with constant S. Moreover, since the static pressure field is coupled to the tangential velocity distribution through the momentum equations and dominates the swirling jet evolution in the near field, vastly different mean jet behavior (e.g., mean centerline velocity decay) should be observable in swirling jets with constant S. To pursue this point further, a unique swirl generator was designed and incorporated in an existing cold jet facility at NASA Lewis Research Center. The mean flow measurement technique employed five-hole pitot probes that compared favorably with the dc signal of a hot-wire anemometer.

The present paper describes the effect of initial swirl distribution on the mean (i.e., time-averaged) evolution of a free turbulent jet. The current investigation is one element of research that fits into our larger objective of achieving active flow control on the turbulent shear layers with swirl. The authors have reported on the preliminary results obtained in a swirling turbulent jet excited by a single-frequency plane wave in Ref. 2.

Review of Literature

From a large body of experimental and theoretical works on the swirling turbulent flows, only a few are selected for the purpose of review in this paper. The bulk of the swirl flow investigations may be categorized, with some interdependence, as follows: 1) swirling turbulent free jet issuing from an orifice into a stationary or moving fluid, 2) confined swirling flows in variable-area ducts (e.g., combustion aerodynamics), 3) swirling flow in turbomachinery annuli, 4) vortex control and management in external/internal aerodynamics, and 5) leading-edge vortex breakdown over a high-angle-of-attack delta wing. The present review concentrates on swirling turbulent free jets with a brief look on the pertinent literature in related areas.

As might be expected, the evolution of a subsonic swirling turbulent jet issuing from a nozzle into ambient fluid depends on the *method* of swirl production. This fact was acknowledged by Chigier and Beér,[3] Pratte and Keffer,[4] and others. The design of swirl generators in practice today use the following principles of swirl production: 1) adjustable vanes, 2) tangential blowing on the wall of a pipe with axial through flow, 3) spinning, fully developed pipe flow emerging from a long rotating tube (~ 100 diam long), and 4) flow through a rotating perforated plate, among others. References 1 and 5 can be consulted on the details of various swirl generator designs and their corresponding limitations and efficiencies.

A number of theoretical studies covering laminar, turbulent, weak, and strong swirling jets have been carried out in the past. Görtler[6] performed analytical studies of an incompressible laminar jet in the limit of very weak swirl. In this limit, the radial pressure gradient may be ignored, i.e., $p = p(x)$ only; moreover, a linearization of the momentum equations in swirl velocity is admissible. Based on these and the boundary-layer approximation of the Navier-Stokes equations, Görtler reduces the evolution of a weakly swirling laminar jet problem to an eigenvalue problem of an ordinary, second-order differential equation. Furthermore, upon finding a suitable transformation for the dependent and independent variables, the governing differential equation is transformed into a Legendre type for which exact solutions are derived. By replacing the kinematic viscosity with an effective constant-eddy viscosity, Görtler generalizes his theory to include turbulent, weakly swirling free jets as well. A theory is proposed by Steiger and Bloom[7] in which incompressible and compressible, axially symmetric laminar free mixing (e.g., wakes and jets) with small, moderate, and large swirl can be examined. The tangential and axial velocity components and the stagnation enthalpy are assumed to have polynomial profiles in the radial direction. The assumption of very small radial velocity allowed the use of boundary-layer-type formulations in the analysis. The von Kármán integral method then is applied to the viscous layer (i.e., the wake) of a rotating axisymmetric body with no comparison to experimental data. Lee[8] has obtained closed-form solutions for an axisymmetric turbulent swirling jet using similarity assumptions for the axial and the tangential velocities. The radial and axial velocities are linked via an entrainment assumption, after Taylor.[9] The theoretical predictions are compared to the experimental data of Rose,[10] where close agreement in the case of weak swirl is demonstrated. The experimental data reported by Rose[10] were collected in a swirling turbulent jet issuing from a long rotating tube. Lee's assumptions of the Gaussian axial velocity distribution and the corresponding similar tangential velocity profile were directly deduced from Rose's experiment, where similarity conditions were observed for $x/D > 1.5$.

Chigier and Chervinski[11,12] have performed theoretical and experimental studies of turbulent swirling jets issuing from a round orifice. They used boundary-layer approximations for assumptions of similar profiles to integrate the equations of motion for incompressible turbulent flows. The similarity assumption was experimentally demonstrated to hold in a swirling jet for weak and moderate swirls, for $x/D > 4$. For strongly swirling flows, where the mean axial velocity distribution shows a central trough, or what is also known as a double-hump profile, the similarity was not observed until 10 diam. For $x/D > 10$, the location of the maximum mean axial velocity shifted back to the jet centerline, from which point the similarity was observed. The measured mean axial velocity and static pressure profiles were described by Gaussian error curves and the mean tangential velocity profile was expressed in terms of third-order polynomials. The empirical constants in the data-fit expressions of Chigier and Chervinsky are functions of the degree of swirl in the jet defined as

$$G \equiv W_{m0}/U_{m0} \tag{4}$$

the ratio of maximum mean tangential-to-axial velocity at the nozzle exit.

Mattingly and Oates[13] performed an experimental investigation of the mean, incompressible mixing process in confined coannular swirling flows. In this investigation, the swirl was present in the inner stream only, thereby leading to flow conditions unstable in the sense of Rayleigh (i.e., instability ensuing from an outwardly decreasing angular momentum). Enhanced radial mixing was attributed to the Rayleigh instability.

The latest reviews in the field of confined swirling flows,[14,15] primarily with combustion, reveal an extensive reference list and activities in this area of research. For a more comprehensive and recent work on the predictions and measurements of the swirling flows in combustor geometries, Ref. 16 may be consulted.

Kerrebrock[17] has proposed a general theory for the small-disturbance field in strongly swirling flows in turbomachine annuli. He concluded that small amplitude "shear" disturbances are not purely convected but rather propagate slowly in flows stable in the sense of Rayleigh and are unstable in flows approaching free vortex.

Extensive literature exists on the phenomenon of vortex breakdown or flow reversal and vortex instability in strongly swirling flows. References 18–20, are among the most fundamental. Despite significant strides, a comprehensive theoretical description of the phenomena leading to vortex breakdown

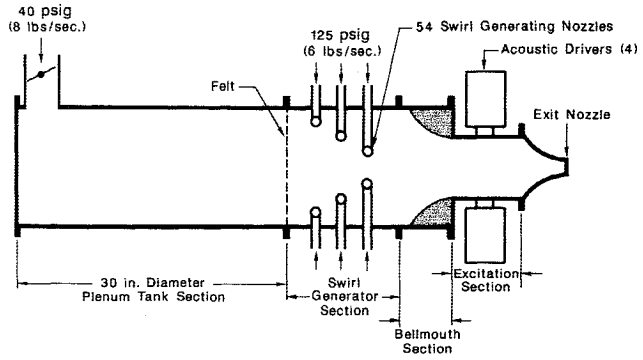

Fig. 1 Schematic diagram of the jet facility.

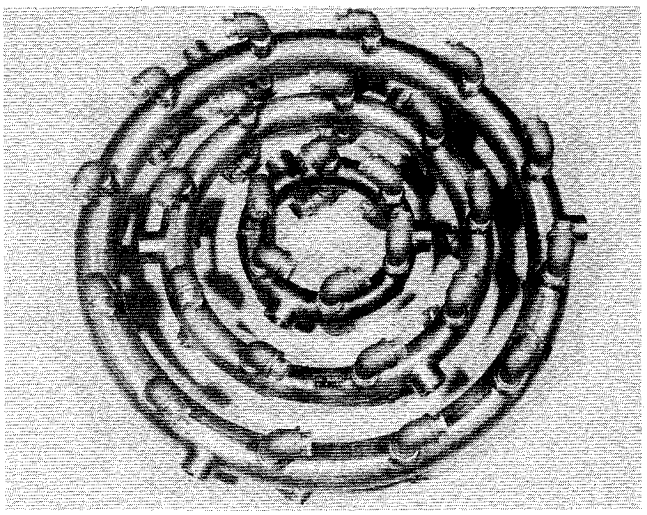

Fig. 2 Manifold rings and elbow nozzles (unassembled).

still does not exist. The various theoretical ideas of hydrodynamic stability and finite transition to a subsequent state (analogous to hydraulic jump) that are proposed provide only partial insight into this complex flow phenomenon. For an exhaustive list of references and critical evaluation of the proposed theories, Refs. 21–23 should be consulted. The special problem of the bursting of leading-edge vortices (e.g., over delta wings) is examined in Refs. 24 and 25. In a recent contribution Shi et al.[26] have experimentally investigated the location and control of vortex breakdown over a delta wing of high sweep angle.

Common to all the previous methods of swirl generation in free jets and ducts, as described in the experimental swirl research articles, is the production of near-solid-body rotation flows. An exception to this is found in a recent contribution by Samimy et al.,[27] who generated forced and free-vortex swirl distributions in their facility. Details of swirl generator design employed by Samimy et al. is described in Ref. 28. In the following section, design of a unique swirl generator system capable of producing variable initial swirl profiles employing the principles of combined tangential and axial air is briefly described.

Experimental Facility

Swirl Generator

Figure 1 is a schematic diagram of the test setup. An existing cold-jet facility at NASA Lewis Research Center was modified to generate flows at a wide range of swirl numbers. The principle of combining axial and tangential streams is applied for swirl generation. Axial air is introduced through a 20.32 cm (8 in.) pipe at the end of the plenum. Tangential air enters the plenum chamber through 54 elbow nozzles mounted on three concentric circular rings as shown in Figs. 1 and 2. Specially

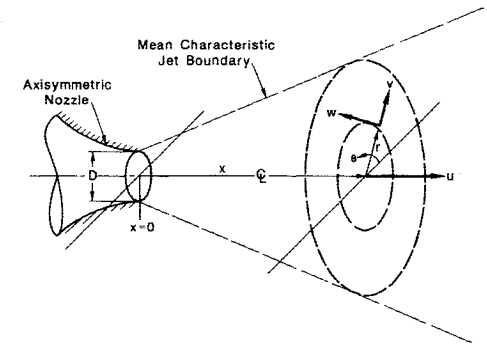

Fig. 3 Definition sketch.

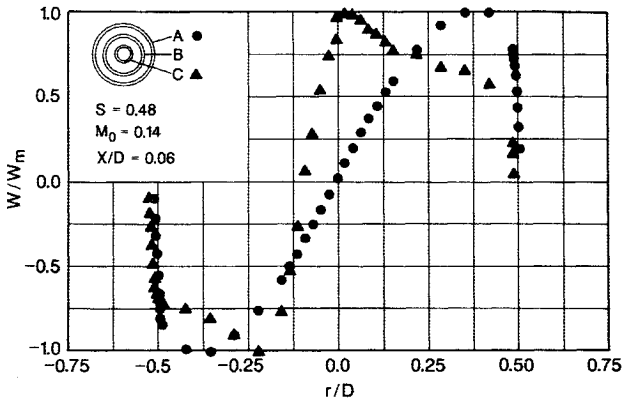

Fig. 4 Radial distribution of the mean tangential velocity.

designed restrictors and screens are inserted into the elbow nozzles to reduce the orifice noise generation. The nozzle exit plane is of a multihole design that also contributes to the nozzles' low-noise character. Swirl number can be adjusted by remote control valves that vary the proportion of axial to tangential air. The flow leaving the swirl generator passes through a bellmouth and an excitation section before discharging to the test cell through an 11.43 cm (4.50 in.) diam nozzle. For more details regarding the swirl generator and test facility, see Ref. 5.

Mean Flow Measurements

Three components of time-mean velocity as well as static and total pressures are measured by a five-hole pitot probe having a diameter of 0.318 cm (0.125 in.). The probe tip has a 45 deg cone angle, and the pressure ports are located at the midspan of the conical surface. The five-hole probe is self-nulling in the yaw angle, while the pitch angle, time-mean velocity components, and pressures are computed from calibration. Mach number range for the five-hole probe varied between 0.08 and 0.4.

Results and Discussion

The experimental results presented in this section are time-averaged data gathered from two swirling jets generated separately by the manifolds A and C. The swirl number in both jets was held constant at 0.48 and the mass-averaged, mean axial Mach number at the nozzle exit was ≈ 0.14. The Reynolds number based on the mean axial velocity and the nozzle diameter was 375,000 in both cases. Figure 3 is a definition sketch showing the coordinates and the mean velocity components in the jet.

The two extreme tangential velocity distributions investigated in our facility are plotted in Fig. 4. The vortex core size generated by the manifold C, at $x/D = 0.06$, is about one quarter of the nozzle exit diameter, whereas that of the manifold A spans across the full exit plane. It also is noted that the center of the smaller vortex is displaced from the nozzle geo-

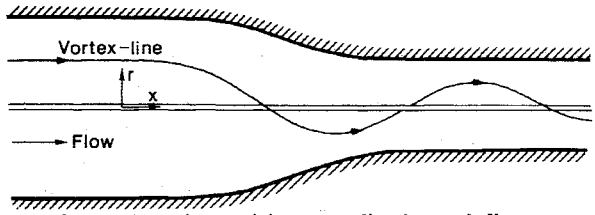

Fig. 5 Conversion of a straight vortex line into a helix on passage through a contraction.

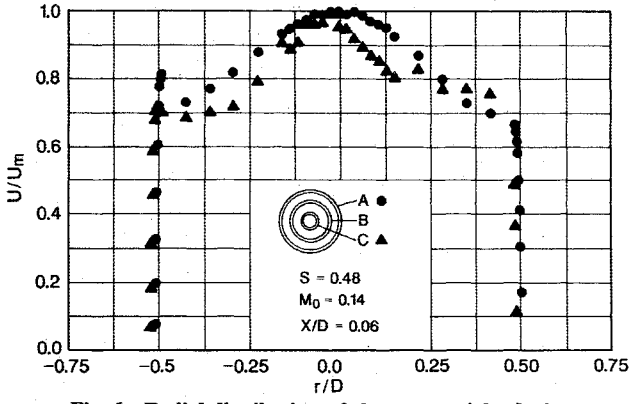

Fig. 6 Radial distribution of the mean axial velocity.

metric center by nearly 0.1 D, at $x/D = 0.06$, thereby leading to nonaxisymmetric flow conditions. This puzzling behavior was further investigated by allowing the vortical flow to emerge from the nozzles of various lengths. It was noted that the vortex core center described a "helical path" as evidenced by the appearance of the vortex center above, below and to the side of the nozzle axis. A plausible explanation of this behavior may be found in the inviscid flow theory; see, for example, Batchelor,[29] who predicts a spiral motion for an off-centered vortex filament as it passes through a contraction. Figure 5 schematically shows this phenomenon. In our case, it seems that manifold C is mounted slightly off center, causing this kind of behavior. The condition of near axisymmetry for the mean swirl distribution in the jet generated by the manifold C is achieved at $x/D \approx 1.0$, as will be discussed later in this section. The forced vortex (i.e., the solid-body rotation flow) produced by the manifold A is axisymmetric as it emerges from the nozzle.

The radial distribution of mean axial velocity is shown in Fig. 6. It is the nature of vortical flows, in general, which do not allow *top hat* axial velocity profiles to be generated. The differences in the axial flow distributions at the nozzle exit produced by the manifolds A and C, as shown in Fig. 6, can be directly related to the size of the vortex cores generated by these manifolds. Furthermore, the condition of near axisymmetry is observed for the swirling jet generated by the manifold A, whereas that of manifold C is still asymmetric.

An evidence of a very strong inward (i.e., negative) radial flow is revealed in Fig. 7 for the swirling flow generated by manifold C. Further, the magnitude of the radial and axial velocity components are comparable in this case in the near field. For example, the ratio of peak radial-to-axial velocity is seen from Figs. 10 and 12b, to be nearly 0.5. Hence, the widely accepted boundary-layer-type approximation, i.e., $V/U \sim \mathcal{O}(\epsilon)$, made in the theoretical analysis of rotating jets is invalid in the *near field* of even moderately swirling jets (e.g., with $S = 0.48$). A manifestation of this assumption, i.e., $V/U \sim \mathcal{O}(\epsilon)$, on the radial momentum equation leads to the radial equilibrium condition, i.e.,

$$-\frac{1}{\rho}\frac{\partial p}{\partial r} = \frac{W^2}{r} \tag{5}$$

which is also invalid for the rotating free jets of the type generated by the manifold C and depicted in Fig. 7 for the near

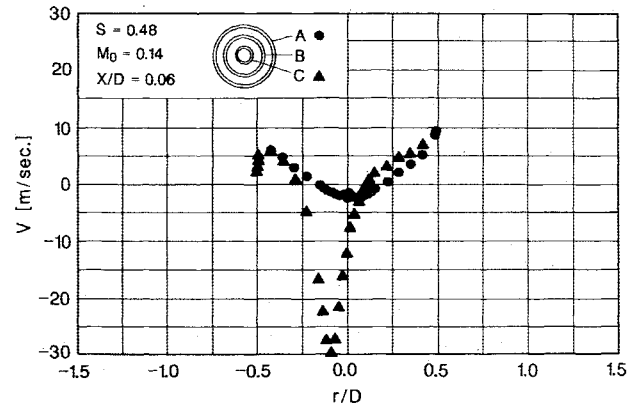

Fig. 7 Radial distribution of the mean radial velocity.

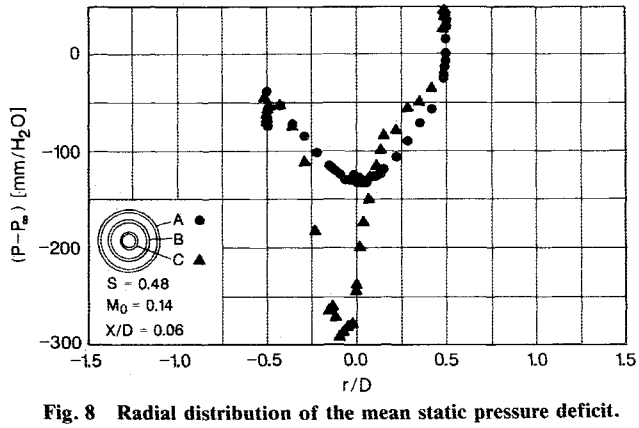

Fig. 8 Radial distribution of the mean static pressure deficit.

field. The driving force behind such a large radial inflow is the radial static pressure gradient associated with the core of such concentrated vortex filaments identifying this as a pressure-driven phenomenon. The axial velocity peak observed in the jet center (see Fig. 6) is the continuity consequence of this radial inflow. The flow generated by the largest manifold (i.e., A) experiences mild radial inflow and is axisymmetric. The rotating flow produced by the smallest manifold (i.e., C) is asymmetric and, as shown in the latter parts of this section, will remain asymmetric in the swirl distribution up to $x/D \approx 1$. Based on physical arguments,[30,31] the inward radial velocity exactly at the vortex center ought to vanish. This feature associated with the vortex core was not resolved, however, with our five-hole probe instrumentation. Currently, a two-component laser Doppler velocimeter (LDV) is under installation in the NASA Lewis free-jet facility that will enable the resolution of the vortex center in our experiments.

Figure 8 reveals a static pressure deficit in the core of the swirling jets, produced by the manifolds A and C, at $x/D \approx 0.06$. The depth of the pressure trough for the concentrated vortex flow (i.e., the one generated by the manifold C) is nearly 2.5 times that of the large core vortex (i.e., due to manifold A). We also note the similarity between the radial velocity and the static pressure profiles as plotted in Figs. 7 and 8. Again, the symmetry and lack of it could be seen in the flows generated by manifolds A and C, respectively.

The axial evolution of the mean tangential velocity is plotted in Fig. 9. In Fig. 9a the swirling flow generated by manifold A is clearly axisymmetric and shows a rapid decay with axial distance. Beyond four nozzle diameters, the mean tangential velocity in the jet is so small as to make an accurate measurement with the four-hole probes questionable. The initial offset between the jet and the nozzle geometric center is clearly visible in Fig. 9b for $x/D < 1.0$. Beyond one nozzle diameter, the two centers coincide. Moving toward the condition of axisymmetry (i.e., the self-centering action of the jet) is a natural tendency we observed in our experiments. How-

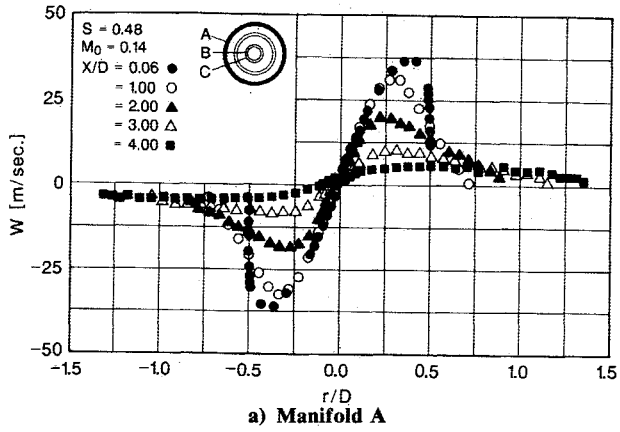

a) Manifold A

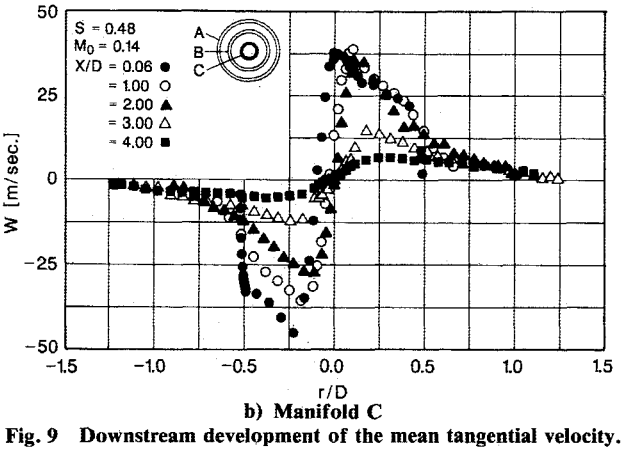

b) Manifold C

Fig. 9 Downstream development of the mean tangential velocity.

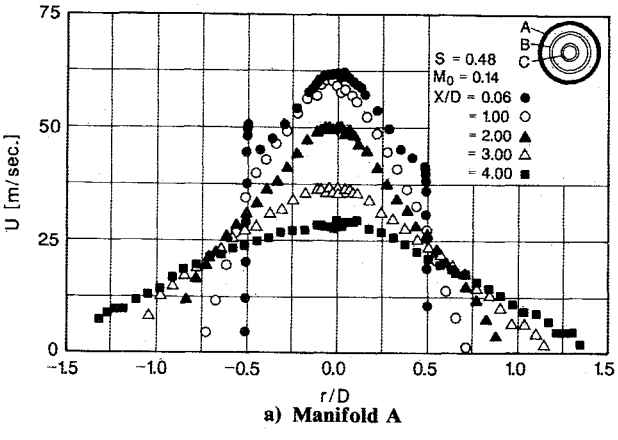

a) Manifold A

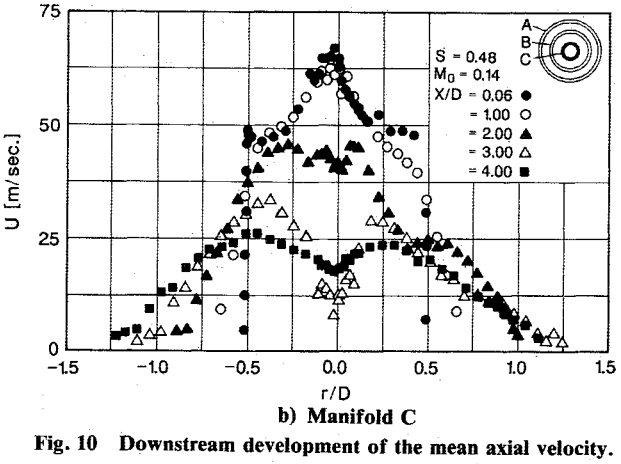

b) Manifold C

Fig. 10 Downstream development of the mean axial velocity.

ever, this is not to be interpreted as the small-core vortex exhibited fully axisymmetric behavior after one nozzle diameter. Only the swirl distribution achieves axisymmetric property for

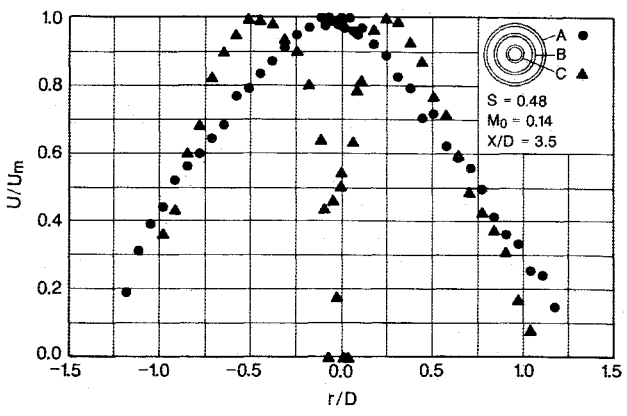

Fig. 11 Radial distribution of the mean axial velocity.

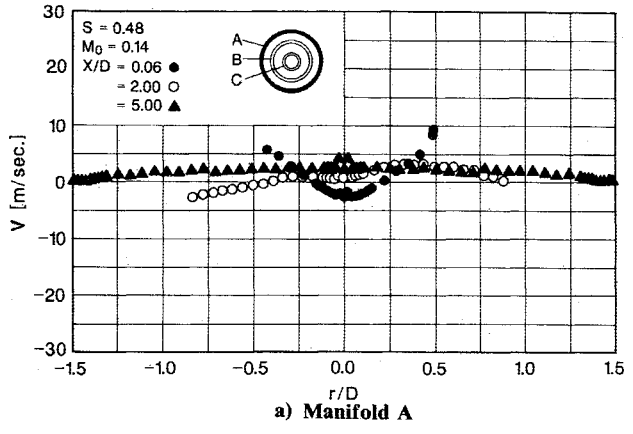

a) Manifold A

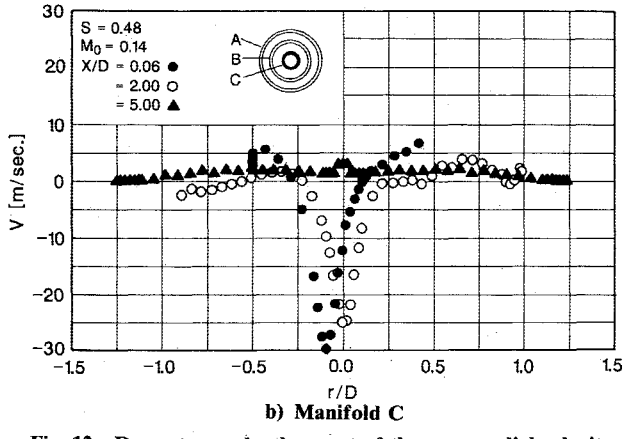

b) Manifold C

Fig. 12 Downstream development of the mean radial velocity.

$x/D > 1.0$, as shown in Fig. 9b. Comparison of Figs. 9a and 9b also reveals that the concentrated vortex (i.e., due to manifold C) decays at a slower rate than the solid-body rotation flow induced by the manifold A, up to four nozzle diameters.

Widely different axial evolution of the mean axial velocity profiles for the two swirling jets generated by the manifolds A and C is noted from Figs. 10a and 10b, respectively. The large-core vortex flow (Fig. 10a) shows a continuous gradual decay of the mean axial velocity component along the jet. The small-core vortex flow (Fig. 10b) demonstrates a central trough or a double-hump profile associated with the swirl numbers higher than 0.48 (namely 0.6). The mean centerline velocity on the jet axis, i.e., $r/D = 0$, in Fig. 10b shows a rapid initial deceleration followed by an acceleration period that has never been reported, to our knowledge, for $S = 0.48$ jets. Upon further examination of the mean axial velocity between three and four nozzle diameters, we observed that the small-core vortex jet with $S = 0.48$ was on the verge of vortex breakdown, as shown in Fig. 11. The forward and rear stagnation points, both very

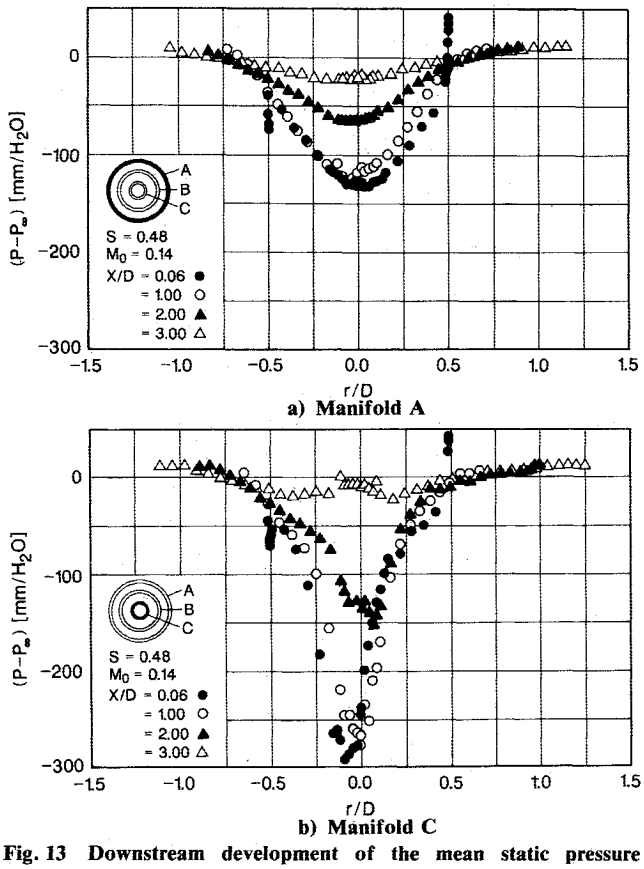

Fig. 13 Downstream development of the mean static pressure deficit.

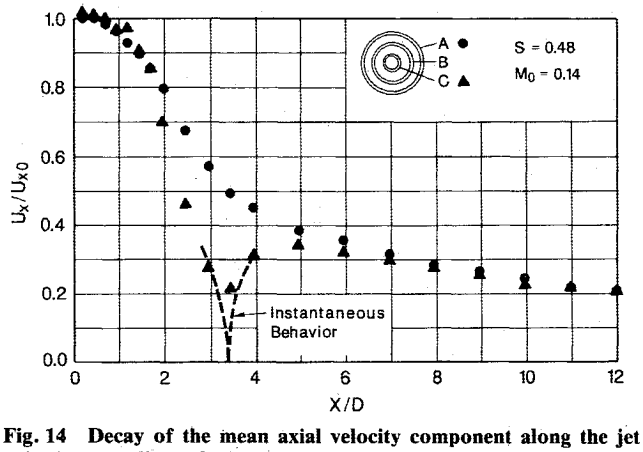

Fig. 14 Decay of the mean axial velocity component along the jet axis (broken lines depict the incipient vortex breakdown at $x/D = 3.5$).

close to the jet axis, exhibited an unsteady behavior, as had been noted in the earlier vortex breakdown experiments. The fact that a swirling jet has been brought to the point of breakdown at a swirl number (i.e., 0.48) significantly lower than the critical value was assumed to be (i.e., $S_{crit} \geq 0.6$) is the most remarkable result of our mean flow investigation. Examining Fig. 10b for the condition of axisymmetry reveals that the mean *axial velocity distribution* associated with the small-core vortex does not achieve near axisymmetric behavior until four nozzle diameters. This is in contrast to the mean *tangential velocity profile,* which exhibited axisymmetric property in one nozzle diameter.

Downstream development of the mean radial velocity is shown in Fig. 12. In Fig. 12a, a very minor radial inflow is measured that quickly disappears as the jet evolves in the axial direction. The small-core vortex flow (Fig. 12b), due to larger inflow radial velocities, persists longer than in Fig. 12a and, as shown, decays to nearly zero radial velocity in about five nozzle diameters. Again we note that the radial velocity at the vortex center must vanish, which the authors could not resolve with the five-hole probe. The mean static pressure deficit in the swirling jet, within the first three nozzle diameters of the jet evolution, is plotted in Fig. 13. The strong adverse pressure gradient along the jet axis, measured for the small-core vortex flow (Fig. 13b) is recognized as the principal contributor to the onset of the vortex breakdown as noted in Fig. 11. Finally, the decay of the mean axial velocity along the jet axis is presented in Fig. 14. The swirling jet produced by manifold C is on the verge of breakdown, while that of manifold A exhibits classical behavior for this level of swirl number, i.e., 0.48. The instantaneous behavior of the incipient vortex breakdown is depicted in Fig. 14 by broken lines. Due to highly unsteady nature of the stagnation point associated with a (bubble-type) vortex breakdown, the time-averaged measurements on the jet axis do not fully resolve this behavior.

Conclusions

An experimental investigation of the effect of initial swirl distribution on the mean evolution of a turbulent jet is performed. The time-averaged jet characteristics in the near field is shown to be significantly influenced by the initial tangential velocity distribution. Swirl number as an integral parameter proves to be insufficient in describing the character of swirling flows. Vortex breakdown, a phenomenon associated with high-intensity swirling flows, is observed at a swirl number ($S = 0.48$) below the "critical value" of $S = 0.6$. The theoretical analysis of free jets with swirl based on the boundary-layer-type approximations and radial equilibrium theory may not be applied to the near-field evolution of a swirling jet with moderate swirl ($S = 0.48$) and small core diameter (relative to the nozzle diameter). Detailed resolution of the flowfield in swirling flows with incipient or fully developed vortex breakdown requires laser-based, nonintrusive, diagnostic instrumentations. Additional nondimensional parameter(s), besides the swirl number, need to be developed to fully characterize the near-field behavior of turbulent flows with general swirl distribution.

Acknowledgments

This research was conducted under NASA Grant NCC 3-56. The authors wish to express their special thanks to Dr. Khairul Zaman, of NASA Lewis Research Center, for his valuable discussion and support.

References

[1]Gupta, A. K., Lilley, D. G., and Syred, N., *Swirl Flows,* Abacus Press, Tunbridge Wells, England, 1984.

[2]Taghavi, R., Rice, E. J., and Farokhi, S., "Controlled Excitation of a Cold Turbulent Swirling Free Jet," *Transactions of the ASME, Journal of Vibration, Acoustics, Stress and Reliability in Design,* Vol. 110, No. 2, April 1988, pp. 234-237.

[3]Chigier, N. A. and Beér, J. M., "Velocity and Static Pressure Distributions in Swirling Air Jets Issuing from Annular and Divergent Nozzles," *Transactions of the ASME, Journal of Basic Engineering,* Vol. 86, Dec. 1964, pp. 788-796.

[4]Pratte, B. D. and Keffer, J. F., "The Swirling Turbulent Jet," *Transactions of the ASME, Journal of Basic Engineering,* Vol. 93, Dec. 1972, pp. 639-748.

[5]Taghavi, R., "Experimental Investigation of Swirling Turbulent Jets," Ph.D. Dissertation, Univ. of Kansas, Lawrence, KS, July 1988 (also NASA CR-180895, March 1988, with S. Farokhi).

[6]Görtler, H., "Decay of Swirl in an Axially Symmetrical Jet, Far from the Orifice," *Revista, Matemática Hispanoaméricas,* Vol. 14, 1954, pp. 143-178.

[7]Steiger, M. H. and Bloom, M. H., "Axially Symmetric Laminar Free Mixing with Large Swirl," *Transactions of the ASME, Journal of Heat Transfer,* Vol. 84-85, Nov. 1962, pp. 370-374.

[8]Lee, S. L., "Axisymmetrical Turbulent Swirling Jet," *Transactions of the ASME, Journal of Applied Mechanics,* Vol. 32, June 1965, pp. 258-262.

[9]Taylor, G. I., "Dynamics of a Mass of Hot Gas Rising in Air," U. S. Atomic Energy Commission, Washington, DC, Rept. MDDC-

919, LADC-276, 1945.
[10]Rose, W. G., "A Swirling Round Turbulent Jet, Part 1: Mean Flow Measurements," *Transactions of the ASME, Journal of Applied Mechanics,* Vol. 29, Dec. 1962, pp. 615-625.
[11]Chigier, N. A. and Chervinsky, A., "Experimental Investigation of Swirling Vortex Motion in Jets," *Transactions of the ASME, Journal of Applied Mechanics,* June 1967, pp. 443-445.
[12]Chigier, N. A. and Chervinsky, A., "Experimental and Theoretical Study of Turbulent Swirling Jets Issuing from a Round Orifice," *Israel Journal of Technology,* Vol. 4, No. 1-2, Feb. 1966, pp. 44-54.
[13]Mattingly, J. D. and Oates, G. C., "An Experimental Investigation of the Mixing of Coannular Swirling Flows," *AIAA Journal,* Vol. 24, May 1986, pp. 785-792.
[14]Syred, N. and Beér, J. M., "Combustion in Swirling Flows: A Review," *Combustion and Flame,* Vol. 23, 1974, pp. 143-201.
[15]Lilley, D. G., "Swirl Flows in Combustion: A Review," *AIAA Journal,* Vol. 15, Aug. 1977, pp. 1063-1078.
[16]Rhode, D. L. and Lilley, D. G., "Predictions and Measurements of Isothermal Flowfields in Axisymmetric Combustor Geometries," NASA CR-174916, May 1985.
[17]Kerrebrock, J. L., "Small Disturbances in Turbomachine Annuli with Swirl," *AIAA Journal,* Vol. 15, June 1977, pp. 794-803.
[18]Benjamin, T. B., "Theory of the Vortex Breakdown Phenomenon," *Journal of Fluid Mechanics,* Vol. 14, 1962, pp. 593-629.
[19]Sarpkaya, T., "On Stationary and Traveling Vortex Breakdown," *Journal of Fluid Mechanics,* Vol. 45, March 1971, pp. 545-559.
[20]Squire, H. B., "Analysis of the Vortex Breakdown Phenomenon," *Miszellaneen der Angewandten Mechanik,* Akademie-Verlag, Berlin, 1960, pp. 306-312.
[21]Hall, M. G., "Vortex Breakdown," *Annual Review of Fluid Mechanics,* Vol. 4, 1972, pp. 195-218.
[22]Leibovich, S., "The Structure of Vortex Breakdown," *Annual Review of Fluid Mechanics,* Vol. 10, 1978, pp. 221-246.
[23]Leibovich, S., "Vortex Stability and Breakdown: Survey and Extension," *AIAA Journal,* Vol. 22, Sept. 1984, pp. 1192-1206.
[24]Lambourne, N. C. and Bryer, D. W., "The Bursting of Leading Edge Vortices; Some Observations and Discussion of the Phenomenon," Aeronautical Research Council, London, R&M 3282, April 1961.
[25]Hall, M. G., "A Theory for the Core of a Leading-Edge Vortex," *Journal of Fluid Mechanics,* Vol. 11, 1961, pp. 209-228.
[26]Shi, Z., Wu, J. M., and Vakili, A. D., "An Investigation of Leading-Edge Vortices on Delta Wings with Jet Blowing," AIAA Paper 87-0330, Jan. 1987.
[27]Samimy, M., Nejad, A. S., Langenfeld, C. A., and Favaloro, S. C., "Oscillatory Behavior of Swirling Flows in a Dump Combuster," AIAA Paper 88-0189, Jan 1988.
[28]Buckley, P. L., Craig, R. R., Davis, D. L., and Schwartzkopf, K. G., "The Design and Combustion Performance of Practical Swirlers for Integral Rocket/Ramjet," *AIAA Journal,* Vol. 21, May 1983, pp. 733-740.
[29]Batchelor, G. K., *An Introduction to Fluid Dynamics,* Cambridge Univ. Press, Cambridge, England, 1967, pp. 543-555.
[30]Marek, C. J., NASA Lewis Research Center, Cleveland, OH, private communication, July 1988.
[31]Abbott, J. M., NASA Lewis Research Center, Cleveland, OH, private communication, July 1988.